Characterization of an amyloid precursor protein-binding protein Fe65L2 and its novel isoforms lacking phosphotyrosine-interaction domains

Hiroshi TANAHASHI[1] and Takeshi TABIRA

Division of Demyelinating Disease and Aging, National Institute of Neuroscience, 4-1-1 Ogawahigashi, Kodaira, Tokyo 187-8502, Japan

Human Fe65L2 is a member of the Fe65 protein family, which interacts with amyloid precursor protein (APP). Fe65L2 contains an N-terminal WW (Trp-Trp) domain followed by two phosphotyrosine-interaction domains, and consists of 486 amino acids. In the present study, we cloned and characterized two novel isoforms of Fe65L2, designated I-214 and I-245, which are produced by alternative splicing of the RNA. The splicing events disrupt the ability to bind with APP and low-density-lipoprotein-receptor-related protein. Fe65L2 was highly expressed in the brain, whereas I-214 and I-245 were expressed in various tissues. In HEK-293 cells, Fe65L2 was expressed in the nucleus and cytosol, whereas I-245 and I-214 were localized exclusively to the nucleus. The ratio of I-214 to Fe65L2 mRNA was increased by apoptotic stimuli. Although the overexpression of either Fe65L2 or I-214 did not significantly affect the half-life and maturation of APP, or the secretion of secreted APP, the secretion of β-amyloid peptide (Aβ)40 and Aβ42 was increased by overexpression of Fe65L2, but not by that of I-214. These results suggest that Fe65L2 affects Aβ production and a possible regulation of Fe65L2 function by alternative splicing.

Key words: alternative splicing, Alzheimer's disease, apoptosis, β-amyloid, low-density-lipoprotein-receptor-related protein (LRP).

INTRODUCTION

Alzheimer's disease (AD) is the most common type of senile dementia and is characterized clinically by a progressive loss of memory and cognitive dysfunction. A pathological hallmark of AD is the cerebral deposition of β-amyloid. β-Amyloid is primarily composed of a β-amyloid peptide (Aβ), 39–43 amino acids in length, which is derived from the proteolytic processing of a 695–770-amino-acid-long amyloid precursor protein (APP) [1]. APP is a cell-surface glycoprotein with a large extracellular N-terminal domain, a single membrane-spanning region and a short cytosolic tail. APP is post-translationally modified and its full-length form is then transported to the plasma membrane where it undergoes processing through alternative proteolysis, secretion, internalization or degradation [2]. One pathway for Aβ production involves the re-internalization of membrane-bound APP into the endoplasmic reticulum and *trans*-Golgi network, which results in the formation of Aβs of different lengths [3,4]. To clarify this mechanism, the network of protein–protein interaction through the cytosolic domain of APP has been studied [5]. The Fe65 family proteins, Fe65, Fe65L1 and Fe65L2 [6–10], bind to the ΦXNPXY motif (where Φ indicates a hydrophobic residue and X, any amino acid) of the cytosolic domain of APP. This motif is believed to be involved in the internalization of cell-surface APP [11]. The Fe65 family proteins have three possible protein–protein-interactive domains, an N-terminal WW (Trp-Trp) domain followed by two phosphotyrosine-interaction domains (PIDs). The C-terminal PID (PID2) of Fe65, Fe65L1 and Fe65L2 interacts with the APP cytosolic domain. One of the family members, Fe65, has been investigated for protein–protein interaction. The N-terminal PID (PID1) of Fe65 interacts with the sequence containing the ΦXNPXY motif in the cytoplasmic tail of the low-density-lipoprotein-receptor-related protein (LRP), an abundant neuronal surface receptor that binds to and internalizes apolipoprotein E, APP and α2-macroglobulin [12]. The WW domain of Fe65 interacts with Mena, a protein that mediates cell-matrix interaction [13]. Thus Fe65 is proposed to be an adaptor protein linking a multi-protein complex to the intracellular domain of APP. Moreover, the effects of Fe65 and/or Fe65L1 in cell cultures on APP maturation, secreted APP (APPs) and Aβ secretion have been reported [14–16]. Genetically, a deletion polymorphism in intron 13 of the Fe65 gene has been reported as having a protective effect in individuals over 75 years of age [17,18] and, recently, we found that the c954C → T polymorphism in the Fe65L2 gene was associated with early-onset AD [19]. In the present work we report two novel isoforms of Fe65L2, designated I-214 and I-245. Fe65L2 was mainly expressed in the brain and localized to the nucleus and cytosol. In contrast, I-214 and I-245 were expressed in various tissues and exclusively localized to the nucleus. Furthermore, secretions of Aβ40 and Aβ42 were induced by overexpression of Fe65L2, but not of I-214. These results suggest distinct roles for Fe65L2 and I-245 or I-214 in Aβ production.

EXPERIMENTAL

Detection of alternatively-spliced transcripts by PCR

cDNA from a human multiple-tissue cDNA panel (Clontech, Palo Alto, CA, U.S.A.), or from various cells, was amplified by PCR (34 cycles of denaturation at 94 °C for 30 s, annealing at 60 °C for 30 s and extension at 72 °C for 30 s) using the human Fe65L2 exon 6 primer 915A, 5′-gagcctagtgaatcccctg-3′ (nt 588–606, GenBank® accession no. AB018247), and primer 620L2, 5′-caaaagcgaagtccctgtca-3′ (antisense of nt 678–697, boundaries

Abbreviations used: Aβ, β-amyloid peptide; AD, Alzheimer's disease; APP, amyloid precursor protein; APPs, secreted APP; CAT, chloramphenicol acetyltransferase; FCS, foetal calf serum; GST, glutathione S-transferase; HA, haemagglutinin; LRP, low-density-lipoprotein-receptor-related protein; MEM, modified Eagle's medium; NES, nuclear export signal; NLS, nuclear localization signal; PID, phosphotyrosine-interaction domain; RT, reverse transcriptase.

[1] To whom correspondence should be addressed (e-mail tanahash@ncnp.go.jp).

of adjacent exons 7 and 8), and the PCR products were electrophoresed on 4% polyacrylamide gels. To detect the full coding sequences of I-214 and I-245, brain cDNA was amplified by PCR (32 cycles of denaturation at 94 °C for 30 s, annealing at 60 °C for 30 s and extension at 72 °C for 1 min) using the primer F0228C, 5′-aagaattcgtt**atg**ctgggcaaggattacat-3′ (the first ATG codon is shown in bold), and the primer 0503B, 5′-aaggatcctgtgggagcacagaagggaatca-3′ (the antisense of a stop codon of I-245 is underlined). The PCR products were subcloned into pT7Blue T-vector (Novagen, Madison, WI, U.S.A.) and sequence analysis was performed.

Measurements of the levels of alternatively spliced transcripts were made in cells that were stimulated by apoptosis-inducing agents. Human neuroblastoma SH-SY5Y, lung fibroblast MRC5 and carcinoma of human cervix HeLa cells were treated with 1 μM staurosporine (Sigma, St. Louis, MO, U.S.A.), 200 μg/ml cycloheximide or 100 μM etoposide (Sigma). Total RNA from the cells was prepared using RNeasy kits (Qiagen, Valencia, CA, U.S.A.) with an RNase-free DNase Set (Qiagen). Single-stranded cDNA was synthesized using a First-strand cDNA Synthesis Kit (Amersham Biosciences, Piscataway, NJ, U.S.A.) with 3 μg of the RNA and random hexamers in 15 μl of reaction mixture. A 1 μl aliquot of the first-strand cDNA was added to 9 μl of PCR reaction mixture containing the primers 915A and 620L2, TaKaRa Ex *Taq*™ Hot Start Version (Takara Shuzo, Otsu, Japan) and 300 kBq [α-^{32}P]dCTP. The PCR products were electrophoresed and analysed with a Fuji BAS 2500 imaging analyser (Fuji photo film, Minami-Ashigara-Shi, Japan). First, to determine the linear range of amplification for both Fe65L2 and I-214, reverse transcriptase (RT)-PCR reactions terminated at 26, 28, 30 and 32 cycles. Since the linearity of amplification over the cycling range (26–32 cycles) for either Fe65L2 or I-214 cDNAs was obtained by semi-logarithmic plots of radioactivity against cycle numbers, we examined the relative levels of I-214 RT-PCR products at 30 cycles in the stimulated cells, compared with those of Fe65L2. For detection of apoptosis of stimulated cells, Western blot analysis was performed using anti-(caspase-3) antibody (BD PharMingen, San Jose, CA, U.S.A.) which recognizes both the 32 kDa pro-caspase-3 and the 17 kDa subunit of the active caspase-3.

Generation of recombinant construct

The entire coding sequences of Fe65L2, I-245, I-214 and Fe65 cDNA and the Fe65 regions from codons 369 to 533 and from codons 242 to 711, tagged with a haemagglutinin (HA)-epitope sequence at the N-terminus, were amplified by PCR and cloned in-frame into pcDNAZeo (Invitrogen, Carlsbad, CA, U.S.A.) for the construction of expression vectors of N-terminal HA-tagged Fe65L2, I-245, I-214, Fe65, Fe65$_{369–533}$ and Fe65$_{242–711}$ respectively. To construct the expression vectors for glutathione S-transferase (GST) fusion proteins of PID1 of Fe65, PID1 of Fe65L2 and C-terminal-truncated PID1 of I-245 or I-214 (GST–Fe65PID1, GST–Fe65L2PID, GST–I-245$_{117–245}$ or GST–I-214$_{117–214}$ respectively), the Fe65 region from codons 369 to 533, the Fe65L2 region from codons 117 to 280, the I-245 region from codons 117 to 245, and the I-214 region from codons 117 to 214 were amplified by PCR and cloned into pGEX4T-1 vectors (Amersham Biosciences) in-frame. To construct a series of yeast GAL4 DNA-binding-domain fusion plasmids, each coding region of Fe65L2 and I-214, the Fe65 region from codons 213 to 445 and the APP695 γ-stab region from codons 637 to 695 were cloned into a pM vector (Clontech) in-frame. To construct a herpes virus VP16 activation-domain–Fe65$_{242–711}$ or –Fe65L2 fusion plasmid, each coding region was cloned into a pVP16 vector (Clontech) in-frame.

Cell culture, transfection, extract preparation and Western blot analysis

HEK-293 cells were cultured in modified Eagle's medium (MEM), supplemented with 10% foetal calf serum (FCS). HEK-293 cells were transfected with pcDNAZeo, pcDNAZeo–HA–Fe65L2, pcDNAZeo–HA–I-254 or pcDNAZeo–HA–I-214 using LipofectAMINE™ 2000 transfection reagent (Life Technologies, Rockville, MD, U.S.A.). At 4 h after transfection, the medium was changed and, at 48 h post-transfection, the cells were harvested. For the preparation of total cell extracts, the cells were sonicated in 65 mM Tris, pH 6.8, and 2.6% (w/v) SDS. Fractionated extracts were prepared essentially as described previously [20], except for the nuclear extract, which was prepared by sonication in lysis buffer [10 mM Hepes, pH 7.9, 1 mM EDTA, 60 mM KCl, 0.2% (v/v) Nonidet P40, 1 mM (*p*-amidinophenyl)methanesulphonyl fluoride HCl, and 10 μg/ml each of aprotinin, pepstatin A and leupeptin] instead of freeze–thaw extraction. The protein concentration was determined by bicinchoninic acid ('BCA') protein assay (Pierce, Rockford, IL, U.S.A.). Each extract (25 μg) was subjected to Western blot analysis using a monoclonal antibody against the HA-epitope, 3F10 (Roche, Mannheim, Germany).

Trans-activation study

Transcriptional effects of Fe65L2, I-214 and Fe65$_{213–445}$ were tested using a pG5CAT reporter vector (Clontech) that contains the chloramphenicol acetyltransferase (CAT) gene downstream of five consensus GAL4-binding sites and the minimal promoter of the adenovirus E1b gene. HEK-293 or HeLa cells in six-well plates were co-transfected with 2.25 μg of pM, pM–Fe65L2, pM–I-214, pM–Fe65$_{213–445}$ or pM3-VP16 positive control vector, which expresses a construct of the GAL4 DNA-binding domain fused to the VP16 activation-domain (Clontech), and 2.25 μg of pG5CAT. To examine the transcription mediated by APP γ-stab fused to the GAL4 DNA-binding domain, cells were co-transfected with 1.5 μg of pM or pM–APP695$_{637–695}$, 1.5 μg of pcDNAZeo, pcDNAZeo–HA–Fe65L2, pcDNAZeo–HA–I-214 or pcDNAZeo–HA–Fe65$_{242–711}$ and 1.5 μg of pG5CAT. At 48 h post-transfection, cells were harvested and the CAT gene expression was measured with a CAT ELISA kit (Roche). The interaction of APP with Fe65 or Fe65L2 was confirmed by the mammalian MATCHMAKER Two-Hybrid assay (Clontech) using pM–APP695$_{637–695}$ and pVP16–Fe65$_{242–711}$ or pVP16–Fe65L2 vector. Western blot analysis using a monoclonal antibody against the GAL4 DNA-binding domain (Clontech) showed that expression levels of each GAL4 fusion protein were similar. CAT values were standardized to β-galactosidase by co-transfection with pCH110 (Amersham Biosciences).

Generation of GST-fusion protein and co-precipitation experiments

GST or GST-fusion proteins were expressed in *Escherichia coli* XLIBlue (Stratagene, La Jolla, CA, U.S.A.) and purified using GSH–Sepharose™ 4B (Amersham Biosciences). A rat liver membrane fraction was prepared as described previously [21]. The membrane pellet was extracted in buffer A (20 mM Tris/HCl, pH 7.5, 2 mM $MgCl_2$, 150 mM NaCl and 1% Triton X-100) containing the protease inhibitors mentioned above. The membrane extract (100 μg) was incubated with 50 μl of 50% (v/v) GSH–Sepharose™ 4B and 10 μg of the respective purified GST-fusion proteins for 6 h at 4 °C. The beads were washed four times

with buffer A and eluted with SDS-sample buffer. The eluted proteins were subjected to Western blot analysis using a monoclonal antibody against the β-chain of LRP, 5A6 (Progen, Heidelberg, Germany).

Metabolic labelling and immunoprecipitation

To analyse the maturation of APP and secretion of APPs, HEK-293 cells that stably overexpressed APP695 [22] were grown in 12-well plates and were transiently transfected with pcDNAZeo, pcDNAZeo–HA–Fe65L2, pcDNAZeo–HA–I-214 or pcDNAZeo–HA–Fe65. At 48 h after transfection, the cells were pre-incubated for 30 min in Met/Cys-free MEM supplemented with 5 % dialysed FCS, after which they were labelled for 15 min with 9.25 MBq [^{35}S]Met/[^{35}S]Cys Pro-mix *in vitro* cell-labelling mix (Amersham Biosciences) per well. The cells were then 'chased' for 15 min, 30 min, 1 h, 2 h or 3 h in MEM supplemented with 10 % FCS. The chase media were collected, spun at 4500 ***g*** for 10 min at 4 °C and supplemented with the protease inhibitors as above. The labelled cells were homogenized in RIPA buffer (50 mM Tris, pH 8.0, 150 mM NaCl, 5 mM EDTA, 1 % Triton X-100, 1 % sodium deoxycholate, 0.1 % SDS) containing the protease inhibitors as above. Insoluble materials were removed by centrifugation at 100000 ***g*** for 1 h at 4 °C. The supernatants or the chase media were pre-cleared with UltraLink™ Immobilized Protein A/G (Pierce). The cell extracts or the media were incubated at 4 °C with 6E10 monoclonal antibody specific for Aβ1-17 (Signet, Dedham, MA, U.S.A.) and UltraLink™ Immobilized Protein A/G for 16 h. The beads were washed four times in RIPA buffer. Immunoprecipitates were eluted by boiling in SDS sample buffer. The eluted proteins were resolved by SDS/PAGE (on 6 % gels), and the gels were dried. The radioactivity in cellular APP or APPs was analysed using a Fuji BAS 2500 imaging analyser. To analyse the secretion of Aβ, the transfected cells (in six-well plates) were labelled for 9 h with 9.25 MBq [^{35}S]Met/[^{35}S]Cys Pro-mix *in vitro* cell-labelling mix per well. The cell extracts or the media were immunoprecipitated with a 6E10 monoclonal antibody, which does not recognize the p3 fragment. The immunoprecipitates were separated by SDS/PAGE (on 6 % gels) for cellular APP or Tris-Tricine SDS/PAGE (on 16 % gels) for secreted Aβ. Aβ radioactivity was normalized to the protein content of the cells, and the mean of the empty-vector-transfected control was set at 100 %.

Sandwich ELISA

HEK-293 cells that stably overexpressed APP695 were transiently transfected with pcDNAZeo, pcDNAZeo–HA–Fe65L2, pcDNAZeo–HA–I-214 or pcDNAZeo–HA–Fe65. At 44 h after the final change of medium, the media were collected, spun at 4500 ***g*** for 10 min at 4 °C and supplemented with protease inhibitors. Aβ sandwich ELISA was performed as described previously [23] using BAN50 as the capture antibody and either horseradish peroxidase-coupled BA27 or BC05 as the detection antibody for Aβ40 and Aβ42 respectively. BAN50 is a monoclonal antibody specific for Aβ1-10 and does not recognize the p3 fragment.

RESULTS AND DISCUSSION

Identification of I-245 and I-214

In the process of isolating the human Fe65L2 cDNA clone [10] (GenBank® accession no. AB018247), we found another cDNA clone. Sequence analysis of this clone showed it to be identical with the Fe65L2 cDNA, except for an additional 36 bp 5′ untranslated sequence, and a 41 bp sequence at the 3′ end of exon 6 was replaced with a 199 bp sequence derived from intron 6. To check if this clone was an artifact of library construction, PCR was performed using a human multiple-tissue cDNA panel and primers from the sequence in exon 6 and boundary sequences of adjacent exon 7 and 8. The PCR produced the 109 bp wild-type band and two larger bands (Figure 1). The PCR products were subcloned into the vector. Sequence analyses of the cloned PCR products revealed the 109 bp wild-type transcript and two alternatively spliced transcripts of 256 bp and 266 bp (Figure 1B). The 256 bp transcript is produced by the use of an alternative-splicing acceptor site in intron 6. The 266 bp transcript is caused by the usage of an alternative-splicing donor site in exon 6 and another acceptor site in intron 6 (Figure 2A). These splicing events lead to unique C-terminal coding sequences and an internal stop codon, resulting in coding sequences of 214 amino acids and 245 amino acids. To confirm the full coding sequences of I-214 and I-245, brain cDNA was amplified by PCR. Electrophoresis of the PCR products showed bands of

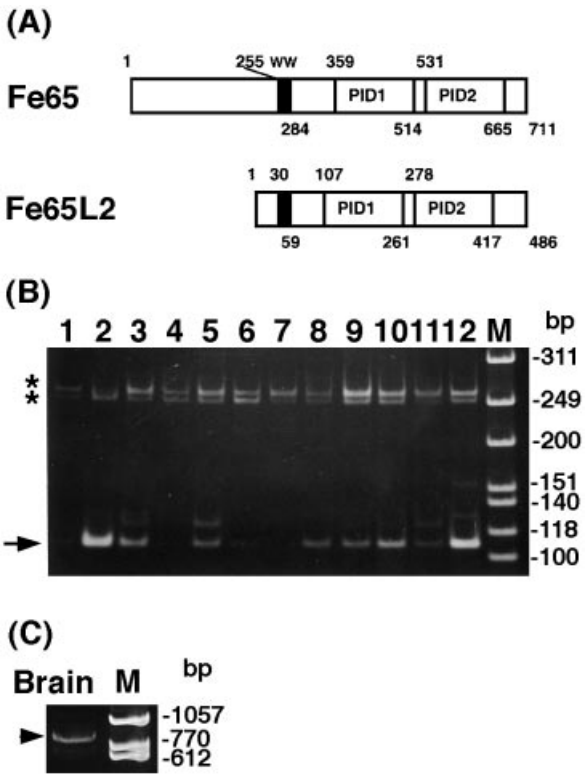

Figure 1 Detection of alternatively spliced transcripts by PCR

(**A**) Domain structure of Fe65 and Fe65L2 with amino acid numbers of domain boundaries. (**B**) cDNA from various tissues and cells was subjected to PCR amplification using the human Fe65L2 exon 6 primer 915A 5′-gagcctagtgaatcccctg-3′ (nt 588–606, GenBank® accession no. AB018247) and primer 620L2 5′-caaaagcgaagtccctgtca-3′ (antisense of nt 678–697, boundaries of adjacent exons 7 and 8). Electrophoresis of the PCR products showed the 109 bp wild-type band (arrow) and two larger (256 bp and 266 bp) bands (*). Lane 1, heart; lane 2, brain; lane 3, placenta; lane 4, lung; lane 5, liver; lane 6, skeletal muscle; lane 7, kidney; lane 8, pancreas; lane 9, HEK-293 cells; lane 10, carcinoma of cervix HeLa cells; lane 11 lung fibroblast MRC5 cells; lane 12, neuroblastoma SH-SY5Y cells; lane M, X174/*Hin*fI size marker. PCR using glyceraldehyde 3-phosphate dehydrogenase showed similar amplification levels among the tissues tested (results not shown). (**C**) To detect the full coding sequences of I-214 and I-245, brain cDNA was amplified by PCR using the primers F0228C and 0503B (see the Experimental section). Electrophoresis of the PCR products showed bands of approx. 770 bp (arrowhead). Sequence analysis of the bands showed the expected full coding sequences of I-214 and I-245. Lane M, X174/*Hin*cII size marker.

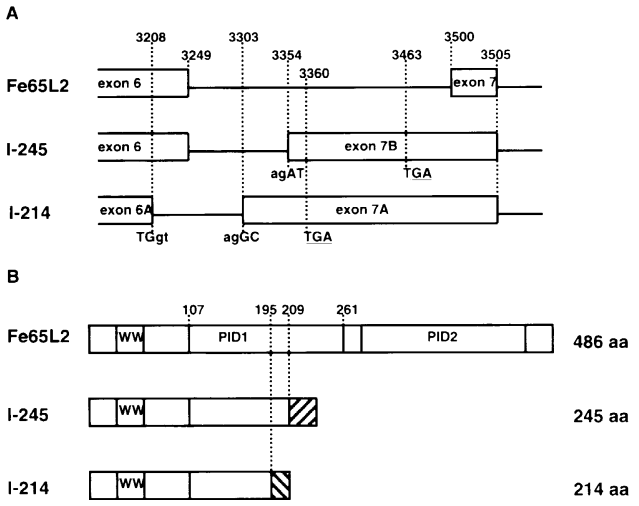

Figure 2 Alternative-splicing variants of Fe65L2

(**A**) Schematic representation of the alternative-splicing site. Boxes indicate exons and solid lines indicate introns. The nucleotide numbering of the ends of each exon is based on GenBank® accession no. AB024745. Sequences of the alternative-splicing site are shown. I-245 is generated by the usage of an alternative-splicing acceptor site in intron 6. I-214 is generated by the usage of an alternative-splicing donor site in exon 6 and another acceptor site in intron 6. These splicing events produce unique coding sequences and an internal stop codon (TGA), and the resultant transcripts encode 214 and 245 amino acids (GenBank® accession nos. AB049618 and AB061224). (**B**) Schematic representation of the alternatively spliced isoforms. I-214 and I-245 lack PID2 and 66 amino acids (43%) and 52 amino acids (34%) of PID1, respectively and have 19 and 36 unique amino acids (hatched rectangles), respectively. Numbers above PID1 indicate amino acid numbers. aa, amino acids.

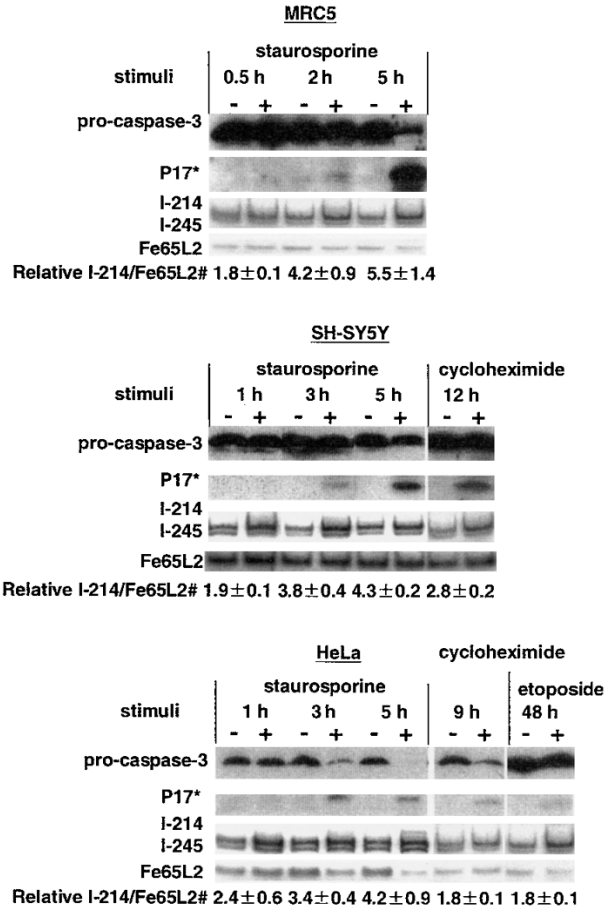

Figure 3 Regulation by apoptotic stimuli of Fe65L2 alternative splice variants

The indicated cell lines were exposed to vehicle (−), 1 μM staurosporine, 200 μg/ml cycloheximide or 100 μM etoposide for the indicated time. Then total RNA was isolated and alternatively spliced Fe65L2 isoforms (Fe65L2, I-214, I-245) were quantified by RT-PCR. # The relative ratio between the value of I-214/Fe65L2 cDNA in the stimulated cells and that in the control cells. The value of the I-214/Fe65L2 in the control cells is set as 1. Results are presented as the means ± S.D. for two (SH-SY5Y and HeLa) or four (MRC5) independent experiments. Apoptosis was induced as indicated by proteolysis of 32 kDa pro-caspase-3 and the 17 kDa subunit (*) of active caspase-3.

approx. 770 bp (Figure 1C). Sequence analysis of the bands showed that the PCR products contain 777 bp and 767 bp fragments, including the expected full-coding sequences of I-214 and I-245. Interestingly, this intron 6, where alternative splicing occurs, is highly similar to the rat intron 6 (200 of 250 nt match, giving 80% identity overall), as we noted previously [24]. Two novel isoforms, designated I-214 and I-245, both lacked PID2. In addition, I-214 also lacked 66 amino acids (43%) of PID1 and had 19 unique amino acids, and I-245 also lacked 52 amino acids (34%) of PID1 and had 36 unique amino acids (Figure 2B). Since the N-terminus of Fe65L2 is very rich in acidic amino acids, I-214 and I-245 are negatively charged (each has a predicted pI of 4.54 or 4.79, whereas that of Fe65L2 is 6.07). In tissues, Fe65L2 mRNA was abundant in brain, and moderate levels of I-214 and I-245 mRNA were expressed in various tissues that were tested, and in human neuroblastoma SH-SY5Y cells, Fe65L2 mRNA was more abundant than I-214 and I-245 (Figure 1). The co-ordinated action of Fe65L2 and its isoforms may contribute to its neuronal function.

The ratio of I-214 to Fe65L2 mRNA was increased by apoptotic stimuli

To investigate whether particular experimental conditions modify the ratio between Fe65L2 RNA and the RNAs of its isoform, MRC5, SH-SY5Y and HeLa cells were treated with a protein kinase inhibitor, staurosporine. Apoptosis was induced, as indicated, by proteolysis of pro-caspase-3. The progression of apoptosis correlated with the increased ratio of I-214 to Fe65L2 cDNA (Figure 3); however the ratio of I-245 to Fe65L2 cDNA was not much changed (results not shown). To investigate whether this effect is limited to staurosporine-induced apoptosis, the cells were treated with further apoptosis-inducing agents, cycloheximide and etoposide. In SH-SY5Y and HeLa cells, cycloheximide- or etoposide-induced apoptosis increased the ratio of I-214 to Fe65L2 cDNA. These results suggest that the ratio between Fe65L2 and I-214 associates with the apoptotic pathway. During apoptosis, a number of kinases are activated [25] and it has been reported that phosphorylation of splicing factors influences alternative splicing [26]. Thus apoptosis stimuli may influence the alternative splicing of the Fe65L2 gene. Whether or not the increased I-214 mRNA contributes to AD neuropathogenesis will be an important consideration for future studies.

Intracellular localization of Fe65L2, I-245 and I-214

To characterize the intracellular localization of Fe65L2, I-245 and I-214, constructs were generated for the expression of N-terminal HA-tagged Fe65L2, I-245 or I-214 and these constructs were transfected into HEK-293 cells. Nuclear and cytosol-

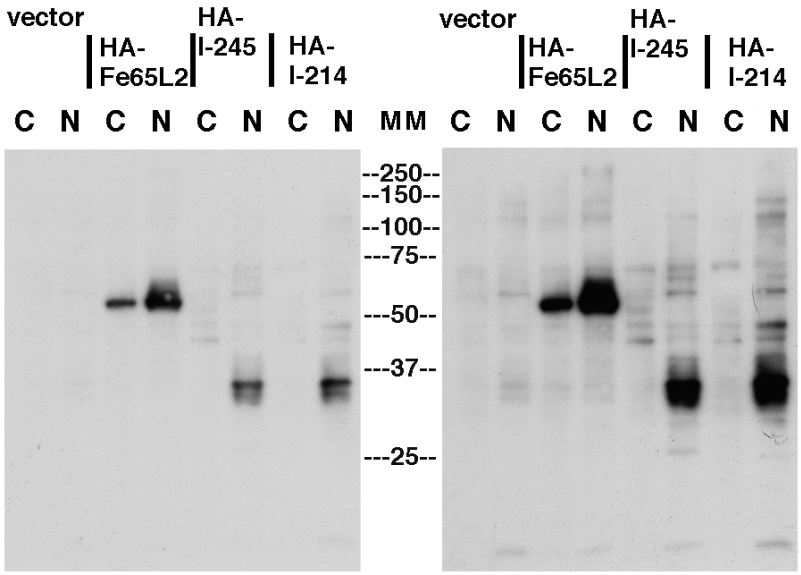

Figure 4 Subcellular distribution of HA-Fe65L2, HA-I-245 or HA-I-214

HEK-293 cells were transfected with pcDNAZeo, pcDNAZeo–HA–Fe65L2, pcDNAZeo–HA–I-254 or pcDNAZeo–HA–I-214. Each fractionated extract (25 μg) was subjected to Western blot analysis using a monoclonal antibody against the HA-epitope, 3F10. N, nuclear fraction; C, cytosol membrane fraction. The right panel shows overexposed film.

membrane fractions were prepared and subjected to SDS/PAGE, followed by Western blot analysis using an anti-HA antibody. Figure 4 shows that transfected HA–Fe65L2 migration was consistent with the predicted molecular mass of 54 kDa, while transfected HA–I-245 and HA–I-214 migrated (at approx. 30 kDa) slightly slower than their predicted molecular masses of 28 and 25 kDa respectively. Interestingly, Fe65L2 was present in both nuclear and cytosol-membrane extracts, whereas I-245 and I-214 were exclusively found in the nuclear extract. A computational analysis of the entire amino acid sequence of Fe65L2, I-245 and I-214 using the PSORT II program [27] revealed no typical consensus sequence for a nuclear export signal (NES), but did indicate a possible nuclear localization signal (NLS) (PRKRGVF) in Fe65L2 at residues 464–470. This, however, is not possible because I-245 and I-214 are exclusively localized to the nucleus. It is possible that they contain other NLSs or NESs, or that they enter the nucleus through an association with other proteins that facilitate access to the transport machinery, as reported for a number of nuclear proteins [28]. Fluorescent microscopy, using a series of deletion mutants of Fe65 fused to green fluorescent protein, showed that Fe65 was mainly present in the nucleus and also localized in the cytosol, and a 100-amino-acid region containing the WW domain is responsible for nuclear translocation and is sufficient to target the nucleus [29]. Furthermore, a deletion mutant lacking PID2 was restricted to the nucleus. The present study shows that alternative-splicing events cause the disruption of two PIDs and generate I-245 and I-214, which retain an intact WW domain having 57% amino acid identity to the WW domain of Fe65 and are restricted to the nucleus. This result is comparable with the above study [29] on Fe65 using deletion mutants.

Table 1 Effect of Fe65L2, I-214 or Fe65 on the transcriptional activation of a CAT reporter gene

HEK-293 (A) or HeLa cells (A and B) were transfected with a CAT reporter plasmid, pG5CAT and each vector set. Results are the means ± S.D. for three to five independent experiments. The value of the empty vector-transfected control is set at 1.

(A)

	Relative CAT activity	
Vector	HEK-293 ($n = 4$)	HeLa ($n = 5$)
pM	1	1
pM–Fe65L2	0.58 ± 0.16	0.57 ± 0.17
pM–I-214	2.17 ± 0.95	5.85 ± 1.56
pM–$Fe65_{213–445}$	2108 ± 595	1469 ± 505
pM3-VP16	2817 ± 925	3618 ± 1388

(B)

	Relative CAT activity
Vector	HeLa ($n = 3$)
pM + pcDNAZeo	1
pM + pcDNAZeo–HA–Fe65L2	0.86 ± 0.11
pM + pcDNAZeo–HA–I-214	0.84 ± 0.09
pM + pcDNAZeo–HA–$Fe65_{242–711}$	0.81 ± 0.31
pM–$APP695_{637–695}$ + pcDNAZeo	1.37 ± 0.14
pM–$APP695_{637–695}$ + pcDNAZeo–HA–Fe65L2	1.17 ± 0.39
pM–$APP695_{637–695}$ + pcDNAZeo–HA–I-214	1.30 ± 0.26
pM–$APP695_{637–695}$ + pcDNAZeo–HA–$Fe65_{242–711}$	91.9 ± 37.00
pM–$APP695_{637–695}$ + pVP16	1.43 ± 0.33
pM–$APP695_{637–695}$ + pVP16–$Fe65_{242–711}$	235 ± 96
pM–$APP695_{637–695}$ + pVP16–Fe65L2	265 ± 110
pM3-VP16 + pcDNAZeo	1174 ± 159

Fe65L2 or I-214 by itself has poor ability for trans-activation

Since Fe65L2 may shuttle between the cytoplasm and nucleus and has multiple protein–protein-interactive domains, there is a possibility that it interacts with other protein partners and participates in an intracellular signal-transduction pathway. A negatively charged N-terminal sequence (amino acids 213–445) of Fe65 has been reported to stimulate GAL4-dependent

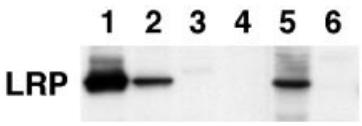

Figure 5 Interaction between the N-terminal PID (PID1) of Fe65L2 and LRP

Membrane extract of rat liver (100 μg) was incubated with 50 μl of 50% (v/v) GSH–Sepharose™ 4B and 10 μg of purified GST-fusion protein for 6 h at 4 °C. Bound proteins were subjected to Western blot analysis using a monoclonal antibody against the β-chain of LRP, 5A6. Lane 1, 25 μg of rat liver membrane extract; lane 2, GST–Fe65L2-PID1; lane 3, GST–I-245$_{117–245}$; lane 4, GST–I-214-PID1$_{117–214}$; lane 5, GST–Fe65-PID1; lane 6, GST.

transcription [30], and Fe65 forms a multimeric complex with the cytoplasmic tail of APP and histone acetyltransferase Tip60 and this complex stimulates transcription [31]. To determine if Fe65L2 can participate in transcriptional activation, Fe65L2 or I-214 was fused to the yeast GAL4 DNA-binding domain cloning vector (pM) and each plasmid was co-transfected with a reporter vector pG5CAT that contains five GAL4-binding sites upstream of a minimal adenovirus promoter which controls the expression of the CAT gene. As expected, Fe65$_{213–445}$ stimulated the transcription strongly (approx. 1400–2100-fold compared with empty-vector transfection). However, Fe65L2 or I-214 caused little transcriptional activation in HEK-293 and HeLa cells (Table 1A). These results suggest that Fe65L2 or I-214 by

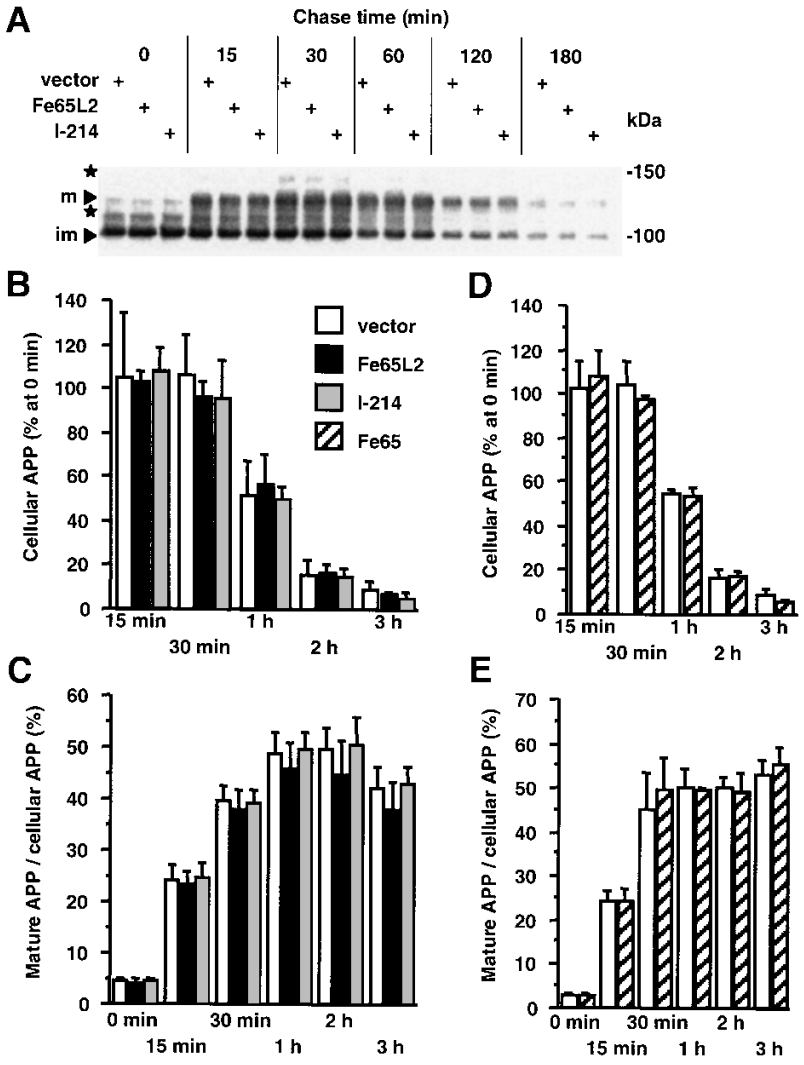

Figure 6 Effect of Fe65L2 and I-214 on the maturation of APP

HEK-293 cells that stably overexpressed APP695 were transiently transfected with pcDNAZeo, pcDNAZeo–HA–Fe65L2 or pcDNAZeo–HA–I-214 (**A**–**C**). The cells were also transiently transfected with pcDNAZeo or pcDNAZeo–HA–Fe65 (**D**, **E**). At 48 h after transfection, the cells were metabolically labelled for 15 min followed by a chase for 15 min, 30 min, 1 h, 2 h or 3 h. Mature and immature APP695 in cell lysates and APPs in conditioned media were immunoprecipitated with an anti-A$\beta_{1–17}$ antibody (6E10) and resolved by SDS/PAGE (6% gel). The radioactivity of mature and immature APP695 was quantified. (**A**) Representative autoradiograms showing the intracellular content of mature and immature APP. Arrows show APP695 mature (m) and immature (im) forms. Asterisks indicate endogenous APP751 isoforms [15]. (**B**, **D**) Kinetics of cellular APP (mature plus immature APP695). The results are expressed as percentages of the cellular APP at chase time zero. The percentage of mature APP (**C**, **E**) was calculated as mature APP695/cellular APP at each time point. Results are presented as the means ± S.D. for four independent experiments.

itself has poor ability for trans-activation. We also examined if overexpression of APP γ-stab ($APP695_{637–695}$) affects the trans-activation of Fe65L2 or I-214 (Table 1B). Co-transfecting HA–$Fe65_{242–711}$ with pM–$APP695_{637–695}$ stimulated transcription approx. 90-fold compared with empty-vector transfection; this result was similar to a previous finding [31]. However, co-transfecting HA–Fe65L2 or HA–I-214 with pM–$APP695_{637–695}$ barely stimulated transcription. The interaction of APP with Fe65 or Fe65L2 was confirmed by the mammalian MATCHMAKER Two-Hybrid assay using pM–$APP695_{637–695}$ and a herpes virus VP16 activation-domain (pVP16)–$Fe65_{242–711}$ or pVP–Fe65L2 fusion vector. Thus the transcriptional effects observed in Fe65 were not found in Fe65L2. Comparison of amino acid sequences between Fe65 and Fe65L2 shows that the sequence upstream of the WW domain and the spacer sequence between the WW domain and PID1 are much shorter in Fe65L2 than in Fe65 (Figure 1A). These results suggest that Fe65L2 or I-214 has a different function from Fe65 in the nucleus.

Fe65L2 interacts with LRP

Previous studies have demonstrated that LRP binds and mediates the endocytosis of soluble, as well as cell-surface, APP isoforms containing a Kunitz proteinase inhibitor domain [32,33], and contributes to the generation of Aβ [34]. The PID1 of Fe65 interacts with the sequence containing the ΦXNPXY motif in the cytoplasmic tail of LRP, and this finding raised the possibility that Fe65 might modulate this endocytic event [12]. Recently, a fluorescence resonance energy transfer study confirmed the intracellular protein interaction between LRP and APP via Fe65 [35]. We addressed whether Fe65L2 interacts with LRP, as Fe65 does. Membrane lysates from rat liver, where LRP is abundantly expressed, were incubated with GST-fusion protein containing PID1 of either Fe65 or Fe65L2 (codons 117–280), or deleted PID1 of either I-245 (codons 117–245) or I-214 (codons 117–214). After adsorption on GSH–Sepharose™ 4B, proteins bound to the beads were separated by SDS/PAGE and analysed by Western blotting with anti-LRP antibodies. LRP was co-precipitated from the liver membrane extract by GST–Fe65-PID1 and GST–Fe65L2-PID1, but not by GST, GST–$I\text{-}245_{117–245}$ or GST–$I\text{-}214_{117–214}$ (Figure 5). Since GST–$I\text{-}245_{117–245}$ and GST–$I\text{-}214_{117–214}$ did not co-precipitate LRP, it is likely that the interaction of Fe65L2 with LRP needs the full PID1 domain. As Fe65L2 and LRP are highly expressed in the brain, Fe65L2 might be involved in the modulation of the endocytic event.

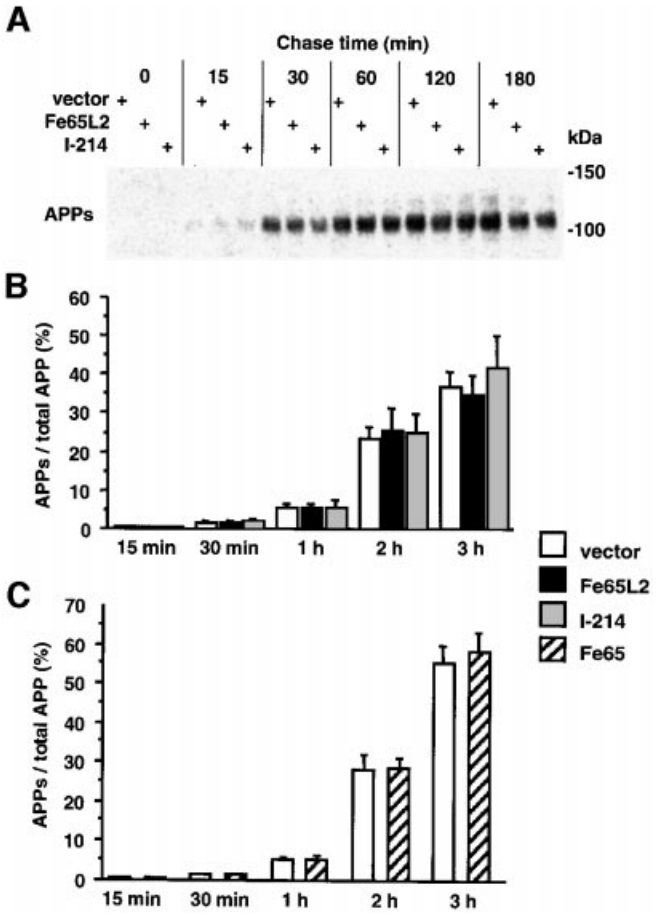

Figure 7 Effect of Fe65L2 and I-214 on the secretion of APPs

HEK-293 cells that stably overexpressed APP695 were transiently transfected with pcDNAZeo, pcDNAZeo–HA–Fe65L2 or pcDNAZeo–HA–I-214 (**A**, **B**). The cells were also transiently transfected with pcDNAZeo or pcDNAZeo–HA–Fe65 (**C**). At 48 h after transfection, the cells were metabolically labelled for 15 min followed by a chase for 15 min, 30 min, 1 h, 2 h or 3 h. APPs in conditioned media were immunoprecipitated with an anti-$A\beta_{1–17}$ antibody (6E10) and resolved by SDS/PAGE (on 6% gels). The radioactivity of APPs was quantified. (**A**) Representative autoradiograms showing the APPs. (**B**, **C**) The percentage of APPs was calculated as APPs/total APP [cellular APP (see Figure 6) plus APPs] at each time point. Results are presented as the means ± S.D. for four independent experiments.

Overexpression of Fe65L2 increased Aβ secretion

We examined whether Fe65L2 affects the maturation of APP or secretion of APPs and Aβ. HEK-293 cells that stably overexpressed APP695 were transfected with pcDNAZeo, pcDNAZeo–HA–Fe65L2 or pcDNAZeo–HA–I-214 and then pulse–chase experiments were performed to study the effect of Fe65L2 and I-214 on maturation of APP and secretion of APPs. The cells were metabolically labelled for 15 min and followed by chase as indicated in Figure 6(A). Mature and immature APP in cell lysates and APPs in conditioned media were immunoprecipitated with an anti-$A\beta_{1–17}$ antibody (6E10) and quantified. As described previously [36,37], APP695 was expressed initially as a 100 kDa immature form, and then processed into a 120 kDa mature form (Figure 6A). Cellular APP695 (mature and immature APP695) levels in transfected cells were similar during the chase period (Figure 6B). The half-life of APP695 was not changed significantly by overexpression of Fe65L2 or I-214 (empty-vector-transfected cell, $t_{1/2} = 65.7 \pm 19.4$ min; HA–Fe65L2 transfected cell, $t_{1/2} = 69.2 \pm 14.8$ min; HA–I-214 transfected cell, $t_{1/2} = 61.8 \pm 6.0$ min). The amount of mature APP695 and APPs was calculated relative to cellular APP and total APP (cellular APP and APPs) at each time point respectively. Neither overexpression of Fe65L2 nor I-214 significantly affected the maturation of APP (Figure 6C) or secretion of APPs (Figures 7A and 7B) at each time point, compared with empty-vector transfection ($P > 0.29$; $n = 4$, unpaired t test). We also examined the effect of Fe65 overexpression on the maturation of APP or secretion of APPs and Aβ, as described above. The half-life of APP695 was not changed significantly by overexpression of Fe65 (empty-vector transfected cell, $t_{1/2} = 66.5 \pm 4.5$ min; HA–Fe65 transfected cell, $t_{1/2} = 65.5 \pm 6.7$ min) (Figure 6D). Overexpression of Fe65 did not significantly affect the maturation of APP (Figure 6E) or secretion of APPs (Figure 7C) at each time point, compared with empty-vector transfection ($P > 0.41$; $n = 4$, unpaired t test). To analyse the secretion of Aβ, the transfected cells were metabolically labelled for 9 h. The labelled cell extracts or the medium was immunoprecipitated with a 6E10 monoclonal antibody and the immunoprecipitates were separated by SDS/

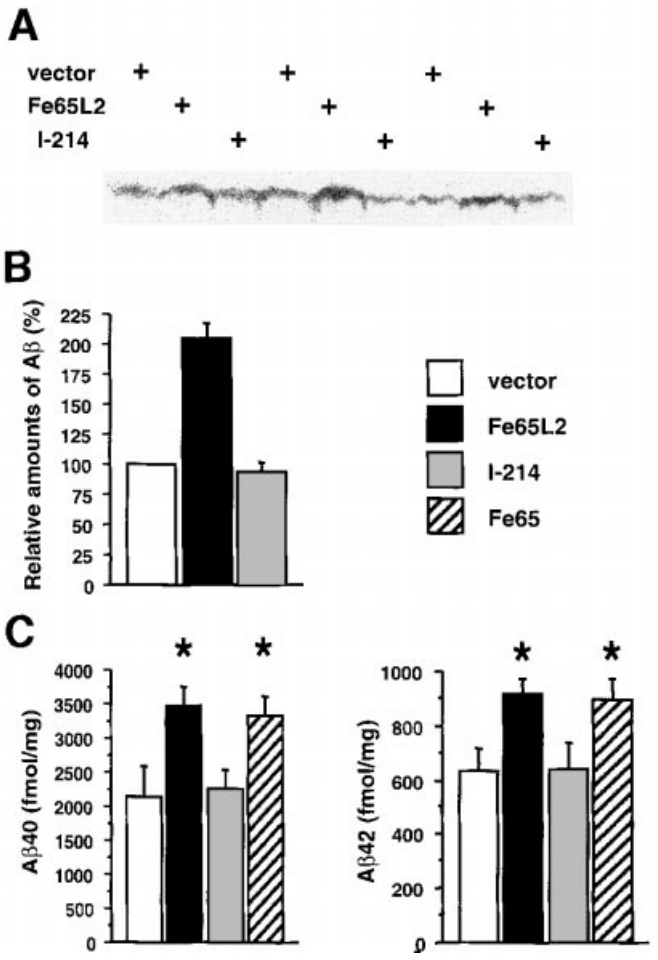

Figure 8 Effect of Fe65L2, I-214 and Fe65 on Aβ production in transiently transfected cells

HEK-293 cells that stably overexpressed APP695 were transiently transfected with pcDNAZeo, pcDNAZeo–HA–Fe65L2, pcDNAZeo–HA–I-214 or pcDNAZeo–HA–Fe65. At 48 h after transfection, the cells were metabolically labelled for 9 h. Aβ in the conditioned medium was immunoprecipitated with an anti-Aβ_{1-17} antibody (6E10) and resolved by Tris-Tricine SDS/PAGE (on 16% gels). Three independent experiments were performed. In each experiment, triplicate samples were measured. (**A**) The autoradiogram represents results typical of those observed in three experiments. (**B**) Aβ radioactivity was normalized to the protein content of the cells, and the mean of the empty vector-transfected control in each independent experiment was set at 100%. Results are presented as means $\pm$ S.D. (**C**) The medium was recovered 48 h after transfection and Aβ sandwich ELISA was performed using BAN50 as the capture antibody and either horseradish peroxidase-coupled BA27 or BC05 as the detection antibody for Aβ40 or Aβ42 respectively. The quantity of Aβ40 and Aβ42 was normalized to the protein content of cells. Results are the means $\pm$ S.D. for four samples. *, $P < 0.005$ compared with pcDNAZeo-transfected cells (unpaired t test).

PAGE (Figure 8A). Cellular APP695 (mature and immature APP695) levels in each transfected cell were similar (results not shown). Overexpression of HA–Fe65L2 increased the secretion of Aβ approx. 2-fold, compared with empty-vector (Figure 8B). However, overexpression of HA–I-214 did not significantly affect the secretion of Aβ. Next, an Aβ sandwich ELISA was performed. Figure 8(C) shows that overexpression of either HA–Fe65L2 or HA–Fe65 increased the secretion of Aβ40 by approx. 62% (3482 ± 271 fmol/mg; $P < 0.005$; $n = 4$, unpaired t test) or approx. 54% (3320 ± 290 fmol/mg; $P < 0.005$; $n = 4$, unpaired t test) respectively, compared with pcDNAZeo-transfected cells (2149 ± 448 fmol/mg; $n = 4$), and increased the secretion of Aβ42 by approx. 45% (916 ± 59 fmol/mg; $P < 0.005$; $n = 4$, unpaired t test) or approx. 42% (898 ± 73 fmol/mg; $P < 0.005$; $n = 4$, unpaired t test) respectively, compared with pcDNAZeo-transfected cells (632 ± 81 fmol/mg; $n = 4$). As expected, overexpression of I-214 did not affect the secretion of either Aβ significantly. Our results relating to the effect of Fe65L2 or Fe65 on APP metabolism differed from previous reports: Fe65 and/or Fe65L1 stimulated the maturation of APP and secretion of APPs and Aβ in Madin–Darby canine kidney and H4 neuroglioma cells [14,15], whereas Fe65 stabilized immature APP and suppressed the secretion of APPs and Aβ in HEK-293 cells [16]. The differences among them may depend on the cells used or the experimental conditions. At any rate, our results suggest that Fe65L2 participates in the production of Aβ and a possible regulation of Fe65L2 function by alternative splicing. Fe65L2 may guide APP to compartments where Aβ is produced, or associate with β-secretase or γ-secretase. Alternatively, Fe65L2 may modulate the endocytic event of APP, resulting in an effect on Aβ generation. Thus these two isoforms may provide a new understanding of the cellular functions of Fe65L2.

We thank Dr N. Suzuki and A. Asami-Odaka (Takeda Pharmaceutical Co., Japan) for providing antibodies BNT-55, BA-27 and BC-05.

REFERENCES

1 Kang, J., Lemaire, H. G., Unterbeck, A., Salbaum, J. M., Masters, C. L., Grzeschik, K. H., Multhaup, G., Beyreuther, K. and Muller-Hill, B. (1987) The precursor of Alzheimer's disease amyloid A4 protein resembles a cell-surface receptor. Nature (London) **325**, 733–736
2 Haass, C. and Selko, D. J. (1993) Cellular processing of beta-amyloid precursor protein and the genesis of amyloid beta-peptide. Cell **75**, 1039–1040
3 Cook, D. G., Forman, M. S., Sung, J. C., Leight, S., Kolson, D. L., Iwatsubo, T., Lee, V. M. and Doms, R. W. (1997) Alzheimer's A beta (1-42) is generated in the endoplasmic reticulum/intermediate compartment of NT2N cells. Nat. Med. **3**, 1021–1023
4 Hartmann, T., Bieger, S. C., Bruhl, B., Tienari, P. J., Ida, N., Allsop, D., Roberts, G. W., Masters, C. L., Dotti, C. G., Unsicker, K. and Beyreuther, K. (1997) Distinct sites of intracellular production for Alzheimer's disease A beta40/42 amyloid peptides. Nat. Med. **3**, 1016–1020
5 Russo, T., Faraonio, R., Minopoli, G., de Candia, P., de Renzis, S. and Zambrano, N. (1998) Fe65 and the protein network centered around the cytosolic domain of the Alzheimer's β-amyloid precursor protein. FEBS Lett. **434**, 1–7
6 Fiore, F., Zambrano, N., Minopoli, G., Donini, V., Duilio, A. and Russo, T. (1995) The regions of the Fe65 protein homologous to the phosphotyrosine interaction/phosphotyrosine binding domain of Shc bind the intracellular domain of the Alzheimer's amyloid precursor protein. J. Biol. Chem. **270**, 30853–30856
7 Zambrano, N., Buxbaum, J. D., Minopoli, G., Fiore, F., de Candia, P., de Renzis, S., Faraonio, R., Sabo, S., Cheetham, J., Sudol, M. and Russo, T. (1997) Interaction of the phosphotyrosine interaction/phosphotyrosine binding-related domains of Fe65 with wild-type and mutant Alzheimer's beta-amyloid precursor proteins. J. Biol. Chem. **272**, 6399–6405
8 Guenette, S. Y., Chen, J., Jondro, P. D. and Tanzi, R. E. (1996) Association of a novel human FE65-like protein with the cytoplasmic domain of the beta-amyloid precursor protein. Proc. Natl. Acad. Sci. U.S.A. **93**, 10832–10837
9 Duilio, A., Zambrano, N., Mogavero, A. R., Ammendola, R., Cimino, F. and Russo, T. (1998) Fe65L2: a new member of the Fe65 protein family interacting with the intracellular domain of the Alzheimer's beta-amyloid precursor protein. Biochem. J. **330**, 513–519
10 Tanahashi, H. and Tabira, T. (1999) Molecular cloning of human Fe65L2 and its interaction with the Alzheimer's beta-amyloid precursor protein. Neurosci. Lett. **261**, 143–146
11 Lai, A., Sisodia, S. S. and Trowbridge, I. S. (1995) Characterization of sorting signals in the beta-amyloid precursor protein cytoplasmic domain. J. Biol. Chem. **270**, 3565–3573
12 Trommsdorff, M., Borg, J.-P., Margolis, B. and Herz, J. (1998) Interaction of cytosolic adaptor proteins with neuronal apolipoprotein E receptors and the amyloid precursor protein. J. Biol. Chem. **273**, 33556–33560
13 Ermekova, K.-S., Zambrano, N., Linn, H., Minopoli, G., Gertler, F., Russo, T. and Sudol, M. (1997) The WW domain of neural protein FE65 interacts with proline-rich motifs in Mena, the mammalian homolog of *Drosophila* enabled. J. Biol. Chem. **272**, 32869–32877

14 Sabo, S. L., Lanier, L. M., Ikin, A. F., Khorkova, O., Sahasrabudhe, S., Greengard, P. and Buxbaum, J. D. (1999) Regulation of beta-amyloid secretion by FE65, an amyloid protein precursor-binding protein. J. Biol. Chem. **274**, 7952–7957

15 Guenette, S. Y., Chen, J., Ferland, A., Haass, C., Capell, A. and Tanzi, R. E. (1999) hFe65L influences amyloid precursor protein maturation and secretion. J. Neurochem. **73**, 985–993

16 Ando, K., Iijima, K., Elliott, J. I., Kirino, Y. and Suzuki, T. (2001) Phosphorylation-dependent regulation of the interaction of amyloid precursor protein with Fe65 affects the production of β-amyloid. J. Biol. Chem. **276**, 40353–40361

17 Hu, Q., Kukull, W. A., Bressler, S. L., Gray, M. D., Cam, J. A., Larson, E. B., Martin, G. M. and Deeb, S. S. (1998) The human FE65 gene: genomic structure and an intronic biallelic polymorphism associated with sporadic dementia of the Alzheimer type. Hum. Genet. **103**, 295–303

18 Lambert, J.-C., Mann, D., Goumidi, L., Harris, J., Pasquier, F., Frigard, B., Cottel, D., Lendon, C., Iwatsubo, T., Amouyel, P. and Chartier-Harlin, M.-C. (2000) A Fe65 polymorphism associated with risk of developing sporadic late-onset Alzheimer's disease but not with Aβ loading in brains. Neurosci. Lett. **293**, 29–32

19 Tanahashi, H., Asada, T. and Tabira, T. (2002) c954C → T polymorphism in the Fe65L2 gene is associated with early-onset Alzheimer's disease. Ann. Neurol. DOI 10.1002/ana.10368

20 Zambrano, N., Minopoli, G., de Candia, P. and Russo, T. (1998) The Fe65 adaptor protein interacts through its PID1 domain with the transcription factor CP2/LSF/LBP1. J. Biol. Chem. **273**, 20128–20133

21 Hubbard, A. L., Wall, D. A. and Ma, A. (1983) Isolation of rat hepatocyte plasma membranes. I. Presence of the three major domains. J. Cell. Biol. **96**, 217–229

22 Tanahashi, H. and Tabira, T. (2001) Three novel alternatively spliced isoforms of the human beta-site amyloid precursor protein cleaving enzyme (BACE) and their effect on amyloid beta-peptide production. Neurosci. Lett. **307**, 9–12

23 Suzuki, N., Cheung, T. T., Cai, X.-D., Odaka, A., Otvos, Jr, L., Eckman, C., Golde, T. E. and Younkin, S. G. (1994) An increased percentage of long amyloid beta protein secreted by familial amyloid beta protein precursor (beta APP717) mutants. Science **264**, 1336–1340

24 Tanahashi, H. and Tabira, T. (1999) Genome structure and chromosomal mapping of the gene for Fe65L2 interacting with Alzheimer's beta-amyloid precursor protein. Biochem. Biophys. Res. Commun. **258**, 385–389

25 Matsuzawa, A. and Ichijo, H. (2001) Molecular mechanisms of the decision between life and death: Regulation of apoptosis by apoptosis signal-regulating kinase 1. J. Biochem. (Tokyo) **130**, 1–8

26 Hartmann, A. M., Rujescu, D., Giannakouros, T., Nikolakaki, E., Goedert, M., Mandelkow, E. M., Gao, Q. S., Andreadis, A. and Stamm, S. (2001) Regulation of alternative splicing of human tau exon 10 by phosphorylation of splicing factors. Mol. Cell. Neurosci. **18**, 80–90

27 Nakai, K. and Horton, P. (1999) PSORT: a program for detecting sorting signals in proteins and predicting their subcellular localization. Trends Biochem. Sci. **24**, 34–36

28 Kaffman, A. and O'Shea, E. K. (1999) Regulation of nuclear localization: a key to a door. Annu. Rev. Cell Dev. Biol. **15**, 291–339

29 Minopoli, G., de Candia, P., Bonetti, A., Faraonio, R., Zambrano, N. and Russo, T. (2001) The beta-amyloid precursor protein functions as a cytosolic anchoring site that prevents Fe65 nuclear translocation. J. Biol. Chem. **276**, 6545–6550

30 Duilio, A., Faffaella, F., Minopoli, G., Zambrano, N. and Russo, T. (1991) A rat brain mRNA encoding a transcriptional activator homologous to the DNA binding domain of retroviral integrases. Nucleic Acids Res. **19**, 5269–5274

31 Cao, X. and Sudhof, T. C. (2001) A transcriptively active complex of APP with Fe65 and histone acetyltransferase Tip60. Science **293**, 115–120

32 Knauer, M. F., Orlando, R. A. and Glabe, C. G. (1996) Cell surface APP751 forms complexes with protease nexin 2 ligands and is internalized via the low density lipoprotein receptor-related protein (LRP). Brain Res. **740**, 6–14

33 Kounnas, M. Z., Moir, R. D., Rebeck, G. W., Bush, A. I., Argraves, W. S., Tanzi, R. E., Hyman, B. T. and Strickland, D. K. (1995) LDL receptor-related protein, a multifunctional ApoE receptor, binds secreted beta-amyloid precursor protein and mediates its degradation. Cell **82**, 331–340

34 Ulery, P. G., Beers, J., Mikhailenko, I., Tanzi, R. E., Rebeck, G. W., Hyman, B. T. and Strickland, D. K. (2000) Modulation of beta-amyloid precursor protein processing by the low density lipoprotein receptor-related protein (LRP). Evidence that LRP contributes to the pathogenesis of Alzheimer's disease. J. Biol. Chem. **275**, 7410–7415

35 Kinoshita, A., Whelan, C. M., Smith, C. J., Mikhailenko, I., Rebeck, G. W. and Hyman, B. T. (2001) Demonstration by fluorescence resonance energy transfer of two sites of interaction between the low-density lipoprotein receptor-related protein and the amyloid precursor protein: role of the intracellular adapter protein Fe65. J. Neurosci. **21**, 8354–8361

36 Oltersdorf, T., Ward, P. J., Henriksson, T., Beattie, E. C., Neve, R., Lieberburg, I. and Fritz, L. C. (1990) The Alzheimer amyloid precursor protein. Identification of a stable intermediate in the biosynthetic/degradative pathway. J. Biol. Chem. **265**, 4492–4497

37 Weidemann, A., Konig, G., Bunke, D., Fischer, P., Salbaum, J. M., Masters, C. L. and Beyreuther, K. (1989) Identification, biogenesis, and localization of precursors of Alzheimer's disease A4 amyloid protein. Cell **57**, 115–126

Received 9 April 2002/29 July 2002; accepted 2 August 2002
Published as BJ Immediate Publication 2 August 2002, DOI 10.1042/BJ20020562